



Proximity Electron Lithography Using Permeable Electron Windows

著者	江刺 正喜
journal or publication title	Applied Physics Letters
volume	91
number	4
page range	044104-1-044104-3
year	2007
URL	http://hdl.handle.net/10097/34840

Proximity electron lithography using permeable electron windows

Wonje Cho, Takahito Ono,^{a)} and Masayoshi Esashi

Graduate School of Engineering, Tohoku University, Aza-aoba 6-6-01, Aramaki, Aobaku, Sendai 980-8579, Japan

(Received 15 May 2007; accepted 29 June 2007; published online 25 July 2007)

This letter reports on an electron source consisting of thin electron-permeable windows and a carbon nanocoil emitter. Electron windows with diameters of 250 nm were fabricated using silicon micromachining technology. Carbon nanocoils that are selectively grown from silicon were used as emitters. Field-emitted electrons from the emitters are transmitted through the thin silicon electron windows with thicknesses in the range of 15–50 nm. The electron transmittance of the electron windows was evaluated and it was demonstrated that transmittances higher than 60% are achievable for the case of electron energies higher than 5 keV. Proximity electron lithography is demonstrated using $1.5 \times 1.5 \mu\text{m}^2$ electron windows with a thickness of 50 nm. © 2007 American Institute of Physics. [DOI: 10.1063/1.2762281]

Electron sources have been used for versatile applications, such as electron microscopy, electron beam lithography, visual displays, etc.¹ In general, the use of high-energy electron sources is limited to vacuum conditions. Therefore, electron windows have been investigated for application to an electron source, in order to provide electrons in atmospheric conditions. Electron windows made of a thin membrane can partially transmit high-energy electrons from a vacuum to the atmosphere. Owing to this characteristic, electron windows have been developed for energy dispersive x-ray spectroscopy and scanning electron microscopy (SEM) in atmospheric applications for portability and interplanetary exploration.^{2,3}

Electron beam lithography with high production throughput is of considerable practical concern due to recent developments in nanofabrication technology. In principle, electron beam lithography can define fine features that are smaller than those using optical lithography, but the throughput is quite low in the case of nanometer size features. Nanoimprint lithography has the capability of defining sub-micrometer patterns, but electron beam lithography is generally required for manufacturing the mold used for nanoimprint lithography. One of the critical issues of electron beam lithography is its low production throughput. In order to improve the throughput, multibeam lithography has been proposed,⁴ but many difficulties associated with the complexity of the multibeam system have to be solved. In this letter, we propose an electron source with electron-permeable micro- and nanowindows for future nanolithography with high production throughput, and a pattern transfer onto an electron beam resist with proximity contact is demonstrated.

Figure 1 shows the concept of the miniature proximity electron source that can be used to emit electrons into the atmosphere from an emitter via electron windows of sub-micrometer to nanometer size. The emitted electrons will be absorbed by the air; therefore, the device is used within a range proximate to the target material. The size of the electron window is much smaller than that of a conventional electron window and, consequently, a small beam near the electron window can be formed easily without complex elec-

tron optics. Electrons are field emitted from the emitters and accelerated by applying a high voltage between cathode and anode. A portion of the electrons then passes through the thin membrane and are emitted into the atmospheric environment. The diameter of the emitted electron beam will depend on the aperture size. Carbon nanocoils (CNCs) were chosen as an emitter material due to their excellent field emission properties.⁵ Silicon carbide (SiC),⁶ silicon nitride (SiN),⁷ and alumina⁸ have been reported as materials used to fabricate electron-permeable windows. The maximum penetration depth of the electrons R into a solid state material depends on the density of the solid and is given by⁹ $R = 4E^2 / c_T \rho m^2$, where E is the electron energy, c_T ($=5.05 \text{ m}^6/\text{kg s}^4$) is the Thomson-Whiddington coefficient, ρ is the density, and m is the electron rest mass. Thus, low density materials are suitable for electron-permeable windows. In addition, this equation can be applied to gas atmospheres. The penetration depth of the ambient atmosphere is approximately 1900 times longer than that of silicon.

In order to increase the electron transmittance, the thickness of the electron windows should be as thin as possible. In this study, we employed single-crystalline silicon (Si) as the material for the electron windows, owing to its high permeability and ease of fabrication in producing an ultrathin Si structure. Si micro- and nanostructures can now be fabricated due to recent advances in microfabrication technology. In addition, single-crystalline silicon has high robustness and low residual stress.

Micro- and nanoelectron windows were fabricated by microfabrication technology. Double silicon-on-insulator (SOI) wafers with a 7- μm -thick first Si layer and a 50-nm-thick second Si layer were prepared using a direct

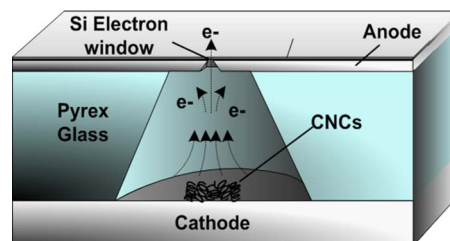


FIG. 1. (Color online) Concept of an electron source with an electron-permeable window.

^{a)} Author to whom correspondence should be addressed; electronic mail: tonono@cc.mech.tohoku.ac.jp

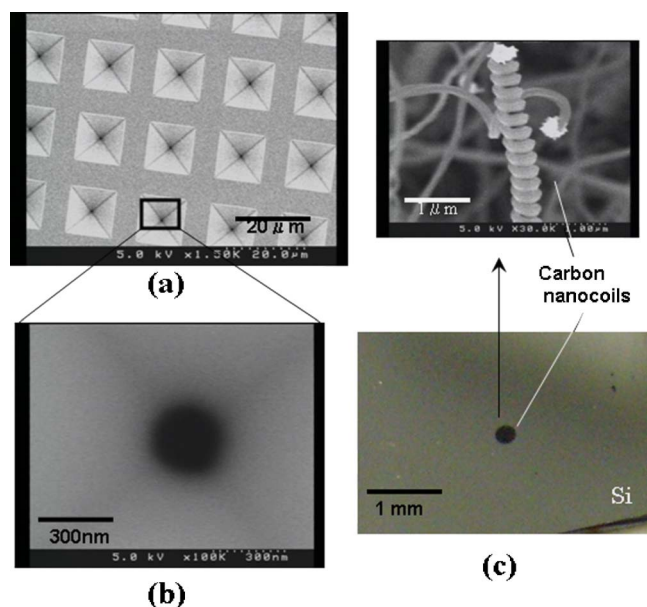


FIG. 2. (Color online) (a) SEM image of fabricated etch pits and (b) SEM image of the electron window at the bottom of the etch pit. (c) Selectively grown carbon nanocoils used as emitters.

wafer bonding technique. Both active layers were made of (100)-oriented single-crystalline Si. After oxidation and photolithography, inversed-pyramidal pits were formed on the top Si layer by anisotropic etching of the Si, and the buried oxide was etched in a hydrofluoric acid solution. Figures 2(a) and 2(b) show typical scanning electron microscopy (SEM) images of the fabricated array of etch pits, and an electron window with a 250 nm diameter at the bottom of the etch pits, respectively. The double SOI substrate was anodically bonded with a 1.6-mm-thick Pyrex glass in which through holes were formed by sandblasting. The handling silicon layer and the buried SiO₂ layer on the top were then removed, leaving a 50-nm-thick membrane on the substrate. As an additional process, the Si membranes were etched by a fast atom beam using SF₆ gas, and electron windows with thicknesses of 30 and 15 nm were fabricated. CNC emitters were selectively grown on the silicon substrate from a catalytic indium tin oxide-iron pattern by thermal chemical vapor deposition using a mixture of acetylene and hydrogen at 700 °C. Figure 2(c) shows the selectively grown CNC pattern on a silicon substrate, and the inset shows a SEM image of the CNCs. The lengths of the most CNCs are ranging from 50 to 100 μm, and the coil diameters are from 100 nm to 2 μm.

The field emission characteristics of the CNCs were measured in an ultrahigh vacuum chamber, and the resulting Fowler-Nordheim (FN) plot is shown in Fig. 3(a). When a voltage was applied between the anode and the emitter, the current flowing into the anode was measured. The measured emission current followed the FN mechanism for field emission.

The electron transmission of an array of 5×5 electron windows with a window size of 1.5×1.5 μm² was also evaluated. A conductive phosphor screen was placed above the electron windows at a distance of 2 mm. A voltage of 3 kV was applied between the CNCs' cathode and anode. An additional voltage of 100 V was also applied to the phosphor screen against the anode, and the transmitted electron current was measured from the current flowing into the screen.

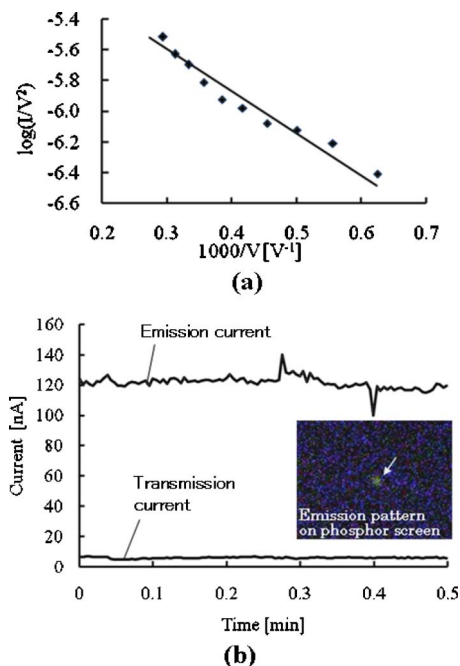


FIG. 3. (Color online) (a) Fowler-Nordheim (FN) plot of the field emission from carbon nanocoils. (b) Time dependence of the field emission current and the transmitted electron current.

Figure 3(b) shows the time dependence of the emission current and the transmitted electron current. The inset shows the fluorescence image of the transmitted electrons. From this figure, it is found that approximately 4% of the electrons emitted from the CNCs are transmitted through the electron window. From this current, the transmitted beam current density at the electron window is calculated to be 90 pA/μm².

Next, the transmittances of individual electron windows were evaluated using SEM. The windows without emitters were placed in a SEM chamber and an electron beam was focused onto one of the grounded electron windows. The electrons transmitted via the electron window were then measured with a Faraday cup. The primary electron current was also measured using the Faraday cup. The transmittance can be calculated from the ratio of the transmitted current to the primary electron beam current. Figure 4 shows the transmittances obtained as a function of the acceleration voltage of the electrons. Measurements were performed on various

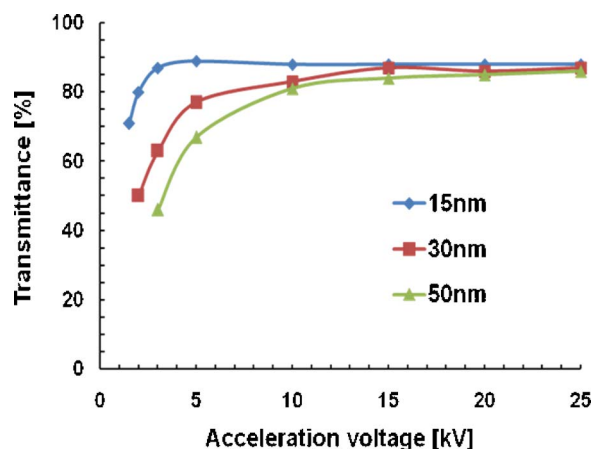


FIG. 4. (Color online) Electron transmittance of silicon windows with thicknesses of 50, 30, and 15 nm.

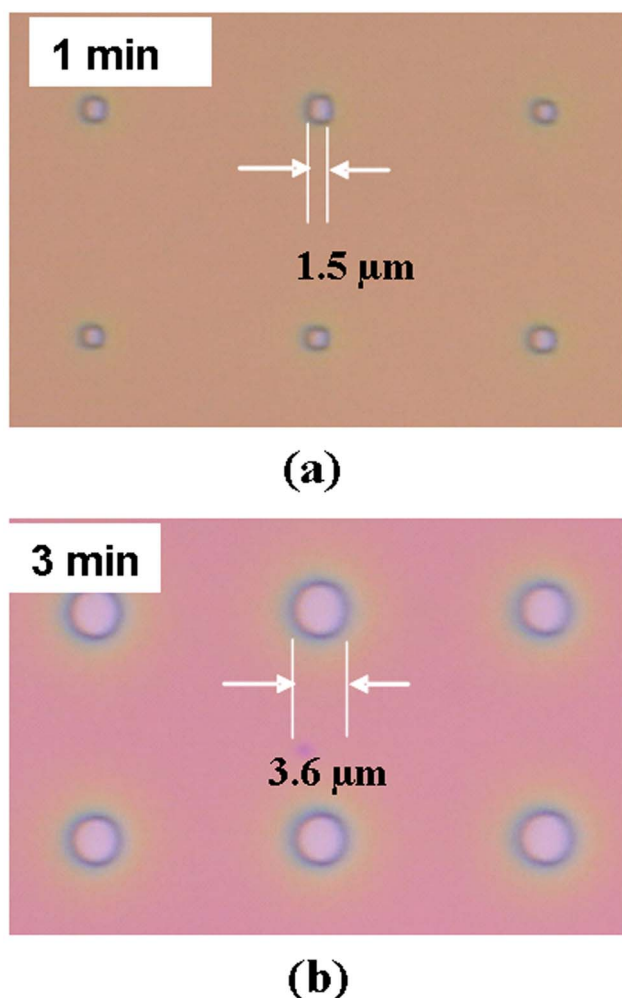


FIG. 5. (Color online) Patterns formed on an electron beam resist using electrons transmitted via silicon electron windows, with an acceleration voltage of 10 kV for 1 and 3 min exposure times.

samples with different window thicknesses. It can be seen that the thinner electron windows exhibit higher transmittance, and quite high transmittance was obtained even at low acceleration voltages.

Electron beam lithography was then demonstrated using the array of 5×5 electron windows with a size of $1.5 \times 1.5 \mu\text{m}^2$ and a thickness of 50 nm. A 350-nm-thick positive electron beam resist (ZEP520A) was spin coated on a silicon substrate and the electron windows were contacted with the substrate in a SEM chamber. The accelerated electron beam was scanned on the electron window array, and the resist was exposed to the electron beam transmitted through the electron windows. Figures 5(a) and 5(b) show examples of the transferred resist pattern with an acceleration voltage of 10 kV and exposure times of 1 and 3 min, respectively. When the primary beam current was 46 pA, the average current density was $3.7 \text{ fA}/\mu\text{m}^2$. If 80% of the electrons are transmitted, then the total dose corresponds to $18 \mu\text{C}/\text{cm}^2$ for the case of a 1 min exposure time. From previous experimental results of the transmittance from CNC emitters, it was determined that a beam current 24 000 times larger can be achieved if nanocoil emitters are used. In addition, the size of the electron windows can be reduced by using a low temperature for the oxidation of Si and etching techniques.¹⁰

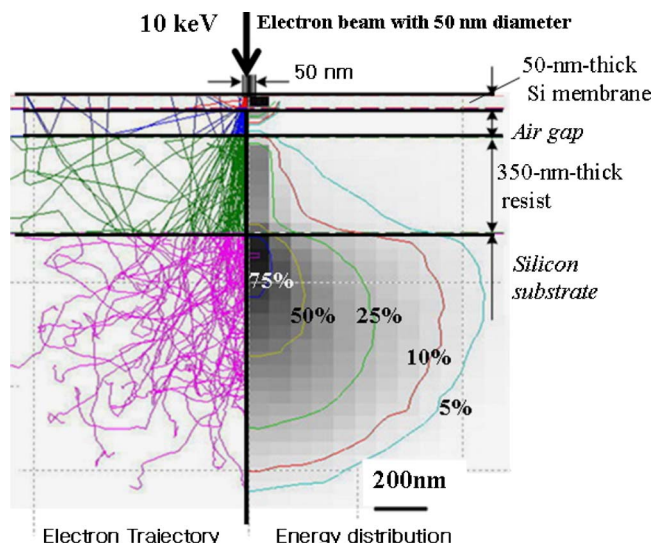


FIG. 6. (Color online) Monte Carlo simulation on electron trajectory (left side) and electron energy distribution (right side).

Figure 6 shows the result of Monte Carlo simulation, which was performed on a model of multilayers with 50-nm-thick Si membrane, 100 nm air gap, and 350-nm-thick resist on a silicon substrate. The left and right sides of the figure show electron trajectory and energy distribution of electrons, respectively. A primary electron beam with a diameter of 50 nm and an energy of 5 keV is irradiated onto the Si membrane. Electrons are slightly scattered and spread in the membrane. However, electron scattering in the air gap is negligible if the gap is enough small. Thinner membrane can reduce the electron scattering and makes electron distribution in the resist small. The detail of the simulation will be described on our future article.

From a technical point of view, each emitter can be electrically isolated and individually operated. It is expected that this electron window device can be applied to high-throughput electron beam nanolithography in ambient atmosphere with scanning of the substrate with a small gap.

Part of this work was performed in the MicroNanomanufacturing Research and Education Center (MNC) of Tohoku University. This work was supported in part by a Grant-in-Aid for Scientific Research from the Japanese Ministry of Education, Culture, Sports, Science and Technology of Japan (No. 21008468 and supported in part by Formation of Innovation Center for Fusion of Advanced Technologies).

¹W. Zhu, *Vacuum Microelectronics* (Wiley, New York, 2001).

²E. D. Green and G. S. Kino, *J. Vac. Sci. Technol. B* **9**, 1557 (1991).

³J. E. Feldman, J. Z. Wilcox, T. George, D. N. Barsic, and A. Scherer, *Rev. Sci. Instrum.* **74**, 1251 (2003).

⁴P. N. Minh, T. Ono, N. Sato, H. Mimura, and M. Esashi, *J. Vac. Sci. Technol. B* **22**, 1273 (2004).

⁵L. Pan, T. Hayashida, M. Zhang, and Y. Nakayama, *Jpn. J. Appl. Phys., Part 2* **40**, L235 (2001).

⁶L. Hanlon, M. Greenstein, W. Grossman, and A. Neukermans, *J. Vac. Sci. Technol. B* **4**, 305 (1986).

⁷F. Hasse, P. Detemple, S. Schmitt, A. Lendle, O. Haverbeck, T. Doll, D. Gnieser, H. Bosse, and G. Frase, *Sens. Actuators, A* **132**, 98 (2006).

⁸T. Doll, M. Hochberg, D. Barsic, and A. Scherer, *Sens. Actuators, A* **87**, 52 (2000).

⁹D. Maurizio, *Electron-beam Interactions with Solids* (Springer, New York, 2003).

¹⁰P. N. Minh, T. Ono, and M. Esashi, *Appl. Phys. Lett.* **75**, 4076 (1999).